Pump and probe spectroscopy with continuous wave quantum cascade lasers

James M. R. Kirkbride,[1] Sarah K. Causier,[1] Andrew R. Dalton,[1] Damien Weidmann,[2] and Grant A. D. Ritchie[1,a)]

[1]*Department of Chemistry, Physical and Theoretical Chemistry Laboratory, The University of Oxford, South Parks Road, Oxford, United Kingdom*

[2]*Space Science and Technology Department, STFC Rutherford Appleton Laboratory, Harwell Oxford Campus, Didcot OX11 0QX, United Kingdom*

(Received 19 November 2013; accepted 20 January 2014; published online 6 February 2014)

This paper details infra-red pump and probe studies on nitric oxide conducted with two continuous wave quantum cascade lasers both operating around 5 μm. The pump laser prepares a velocity selected population in a chosen rotational quantum state of the $v = 1$ level which is subsequently probed using a second laser tuned to a rotational transition within the $v = 2 \leftarrow v = 1$ hot band. The rapid frequency scan of the probe (with respect to the molecular collision rate) in combination with the velocity selective pumping allows observation of marked rapid passage signatures in the transient absorption profiles from the polarized vibrationally excited sample. These coherent transient signals are influenced by the underlying hyperfine structure of the pump and probe transitions, the sample pressure, and the coherent properties of the lasers. Pulsed pump and probe studies show that the transient absorption signals decay within 1 μs at 50 mTorr total pressure, reflecting both the polarization and population dephasing times of the vibrationally excited sample. The experimental observations are supported by simulation based upon solving the optical Bloch equations for a two level system.
 [http://dx.doi.org/10.1063/1.4864001]

I. INTRODUCTION

High power continuous wave (cw) quantum cascade lasers (QCLs) open up the possibility for coherent rovibrational state preparation of gas phase molecules in low frequency vibrational modes.[1–3] For example, McCormack *et al.* recently presented a study in which a single mode QCL operating at 10 μm was used to record absorption spectra of low pressure samples of carbonyl sulphide in an astigmatic Herriott cell.[4] As a result of the frequency chirp of the laser and the low collision rate within the sample, the spectra show the effects of rapid passage (RP) on the absorption line shape.[5–7] The corresponding simulated transient absorption profiles showed good quantitative agreement with those measured experimentally over a range of chirp rates and optical thicknesses. At a chirp rate of 0.13 MHz ns^{-1}, the calculated population transfer between rovibrational quantum states using an overtone transition is 12%, considerably larger than that obtained at the higher chirp rates produced by pulsed QCL experiments.[8] Population transfer in a low pressure sample of nitric oxide (NO) has been shown to be chirp rate dependent with a cw QCL.[9] In that study 35% population transfer was achieved and RP structure observed within Lamb-dip spectra. Other coherent phenomena may also be observed with rapidly chirped cw QCLs and particularly striking is the work by Duxbury *et al.*,[10,11] demonstrating the electric field induced Autler-Townes splitting in NO. In this case the splitting, observed in a low pressure sample of NO over a path-length of 100 m, was also found to be chirp rate dependent.

Pursuing these studies of coherent effects using dual laser pump and probe approaches, the population transfer induced by a cw QCL pump operating at 5 μm in a low pressure of NO was directly probed by another cw QCL in a counter-propagating arrangement.[12] In this case, the strong pump field excites a fundamental rovibrational transition and the weaker probe field is tuned to an appropriate rotationally resolved hot band transition. When both light fields are in resonance, RP is observed in the hot band absorption lineshape arising from a minimally damped and velocity-selected sample of molecules in the $v = 1$, J state. In those first experiments a commercial external cavity QCL (140 mW of optical power and a linewidth of 2 MHz) was used as the pump laser while the probe laser was a distributed feedback QCL (7 mW of power and a linewidth of 16 MHz).

For this work, the weak probe has been replaced with a higher powered (up to 250 mW) and significantly narrower bandwidth (800 kHz) device. The corresponding pump and probe investigation are hereby presented. As in Ref. 12, a velocity group is selected, and RP signals show the effect of improved lasing properties of the probe. The influence of gas pressure, laser power, and chirp rate on the RP signals is systematically studied. In addition, the dephasing rates of the RP signals are shown to be subtly different for each Λ-doublet of the probed rovibrational states indicating that the apparent dephasing time of the coherent transient signal is affected by the underlying hyperfine structure.[13,14] The time scale for the combined polarization and population relaxation of the

a)E-mail: grant.ritchie@chem.ox.ac.uk

system is further investigated by measuring transient data with an amplitude modulated pump field. All of the experiments reported utilize rotationally resolved transitions within the $v = 1 \leftarrow 0$ and $2 \leftarrow 1$ vibrational bands of the $^2\Pi$ ground electronic state of NO at $\sim 5\ \mu$m. The transitions are denoted as $\Delta N(J)_\Omega$, where N is the initial rotational quantum number, J is the total angular momentum quantum number ($J = N \pm 1/2$), and $\Omega = 1/2;3/2$ defines the spin-orbit state.

II. EXPERIMENTAL

The two lasers employed in this work are (1) a commercial cw external cavity quantum cascade laser (Daylight Solutions) covering 1776 to 1958 cm^{-1} that emits up to 140 mW of optical power and exhibits a linewidth of $\approx$2 MHz,[15–17] and (2) a distributed feedback cw QCL (Maxion Technologies M575AH-NS) covering 1897–1904 cm^{-1}, with up to 250 mW of optical power and a linewidth of $\approx$800 kHz.[4] The distributed feedback (DFB) laser resides in an in-house designed mount cooled by a two stage Peltier thermoelectric cooler and is driven by a custom designed low noise current source. The two laser beams counter-propagate with a small uncrossing angle ($\sim 0.5^\circ$) through an 84 cm long absorption cell containing a low pressure of NO gas (5–500 mTorr). After passing through the cell both beams are focussed by off-axis parabolic mirrors onto two 20 MHz bandwidth thermoelectrically cooled mercury cadmium telluride detectors (VIGO PVMI-3TE-10.6 and VIGO PVI-2TE-6, respectively), see Figure 1.

When the external cavity (EC) QCL was used as the pump laser, its frequency was scanned by applying a sine wave modulation (at a frequency in the range 5 to 40 Hz) to the piezo-electric transducer (PZT) attached to its external grating. This modulation signal was derived from a TTi function generator (TG230) and resulted in (near) linear laser chirp rates in the range 20 to 150 Hz ns^{-1} (measured using a 500 MHz etalon). In this case, a triangular current modulation was then applied to the DFB laser using a second TTi function generator (TG1304) with frequency ramps selected from the range 10 kHz to 75 kHz. Within a single current sweep, the total frequency scan range was 1.6 GHz, producing chirp rates ranging from 30.5 kHz ns^{-1} to 265.5 kHz ns^{-1}. The three orders of magnitude ratio between the two laser chirp rates implies that the pump laser remains quasi-static during a single frequency scan of the probe laser. In some experiments the roles of each laser were reversed and the corresponding chirping conditions will be presented later in the text as appropriate. The absorption signals from both lasers are collected and recorded by a 2.5 gigasample/s, 400 MHz bandwidth digital oscilloscope (LeCroy Wavesurfer 44MXs-A). During each frequency scan of the pump laser, which encompasses the fundamental absorption transition, a pre-selected number of probe laser scans are recorded and averaged. The data analysis method employed is presented in Sec. III.

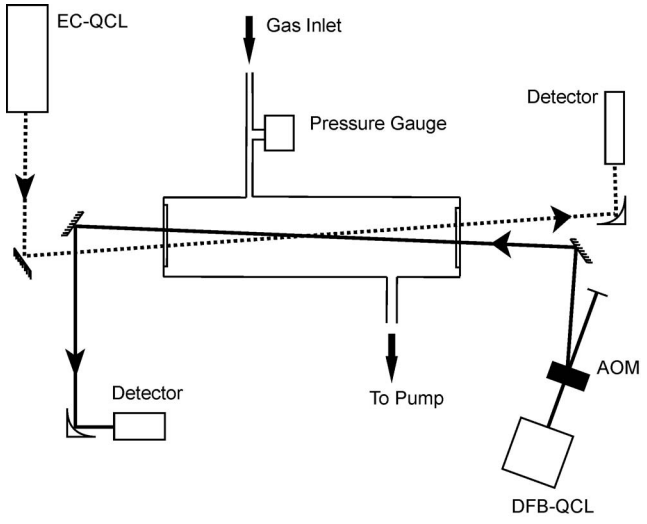

FIG. 1. Schematic of the experimental setup.

For some of the later experiments the pump laser was amplitude modulated using an acousto-optic modulator (AOM, Isomet 1208-6-4M) as a fast optical switch. In this case a digital function generator (TTi TG1304) provided a square wave voltage input to the radio-frequency driver (Isomet RFA151) which output a 50 MHz signal to the AOM PZT thereby creating acoustic waves within a germanium crystal. When directed through the crystal the pump beam is split into two beams corresponding to the zeroth order and the frequency-shifted first order. As shown in Figure 2(a) the time scale over which the AOM transmission of the first-order beam rises from zero to full power was measured to be 506 ± 9 ns, in close agreement with the manufacturers' specification. The frequency offset between the zeroth and first-order beams should be 50 MHz and this was confirmed by the following experiment: the EC-QCL output, resonant with the fundamental $R(6.5)_{1/2}$ transition, was directed into the AOM, and two Bennett holes were burnt into a low pressure NO sample using both the zeroth and first-orders of the modulated EC-QCL beam. The Bennett holes were observed by aligning both orders with the counter-propagating DFB probe which was scanned across the same $R(6.5)_{1/2}$ transition. A frequency scale was set using the known separation of the $R(6.5)_{1/2}$ Λ-doublet components so that the 50 MHz offset between the zeroth and first orders could be experimentally verified as 49.6 ± 0.9 MHz. The widths of the Bennett holes shown in Figure 2(b) correspond to the pump laser linewidth of $\sim$2 MHz, and demonstrate that the AOM does not change the linewidth of the modulated IR radiation. The pump power was attenuated by varying the voltage supplied to the AOM and thus the proportion of photons deflected into the first-order beam. It should be noted that power attenuation by this method does not change the laser linewidth or polarisation and therefore offers a distinct advantage over power tuning by injection current modulation or use of a polariser.

III. RESULTS AND DISCUSSION

A. Rapid passage from a velocity selected sample

In all of the experiments, the pump and probe lasers share a common intermediate state. As a first example, consider the case where the $R(14.5)_{1/2}$ $v = 1 \leftarrow 0$ transition of NO was pumped using the EC-QCL while the DFB laser probed the

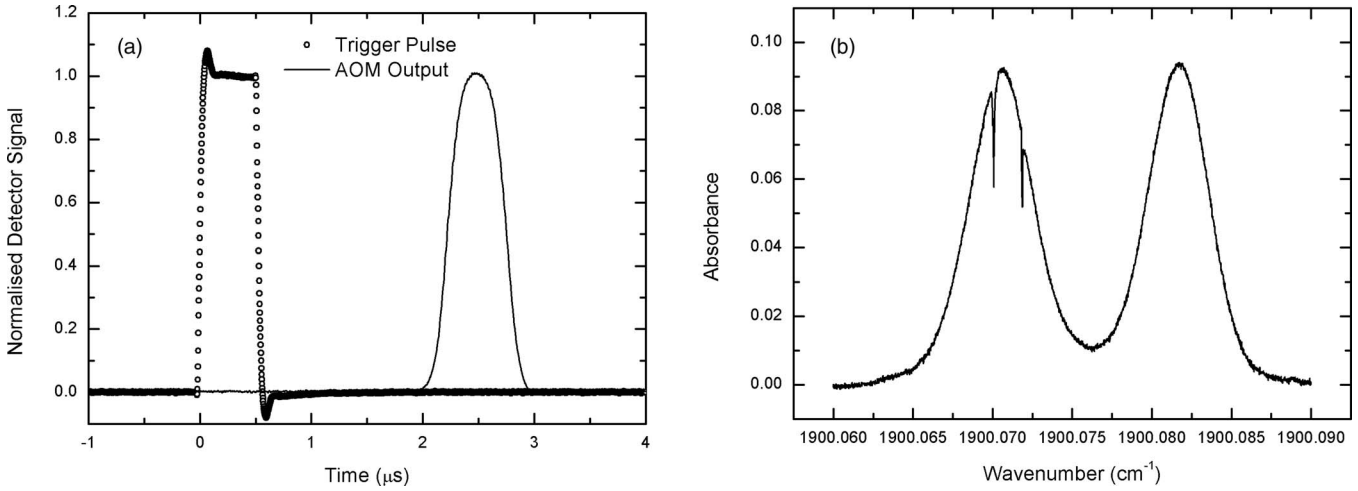

FIG. 2. (a) AOM output pulse produced by applying a 0.5 μs trigger pulse to the driver and (b) two Bennett holes in the Doppler profile of the R(6.5)$_{1/2}$ $v = 1 \leftarrow 0$ transition of NO showing the frequency offset between the zeroth and first order beams transmitted through the AOM. The first order beam burns the hole at the higher frequency.

R(15.5)$_{1/2}$ $v = 2 \leftarrow 1$ transition. Figure 3 shows the multiple scans of the probe laser as the pump laser is tuned slowly over the Doppler profile of the fundamental transition. The data shown are obtained at a pressure of 50 mTorr. Throughout the Doppler broadened absorption profile, the narrow bandwidth (~2 MHz) pump laser excites a particular velocity group within the NO gas sample into the $v = 1$ level. As shown in Figure 3i–iii, the magnitude of the transient absorption signals

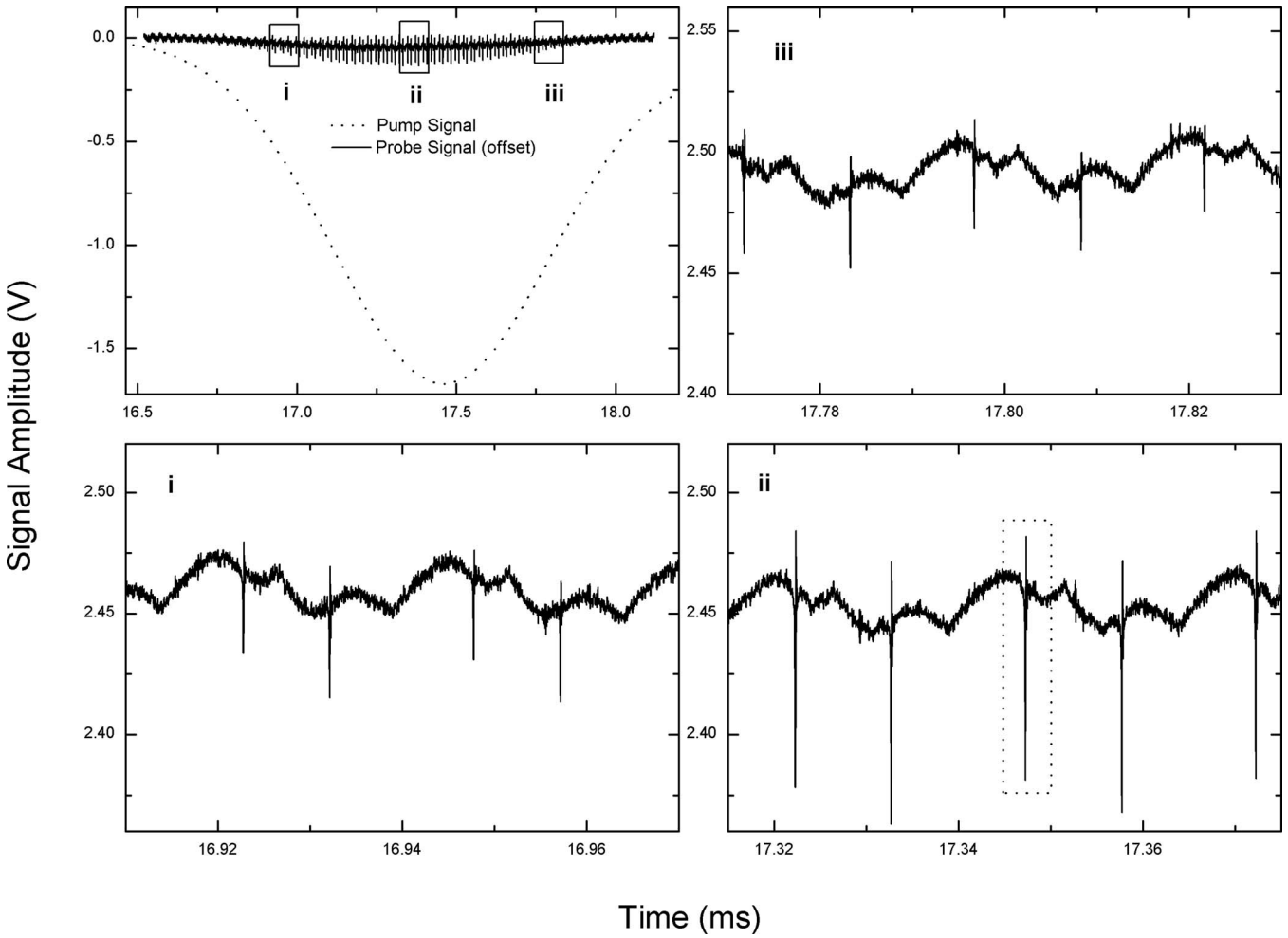

FIG. 3. Example signals obtained from the probe scan as the pump laser is slowly tuned across the Doppler profile of the R(14.5)1/2 $v = 1 \leftarrow 0$ transition of NO. The amplitude of the rapid passage signals mirrors the instantaneous magnitude of the absorbance of the pump. The data shown were taken at a pressure of 50 mTorr. A zoom in of the data highlighted in "ii" will be presented in Figure 4.

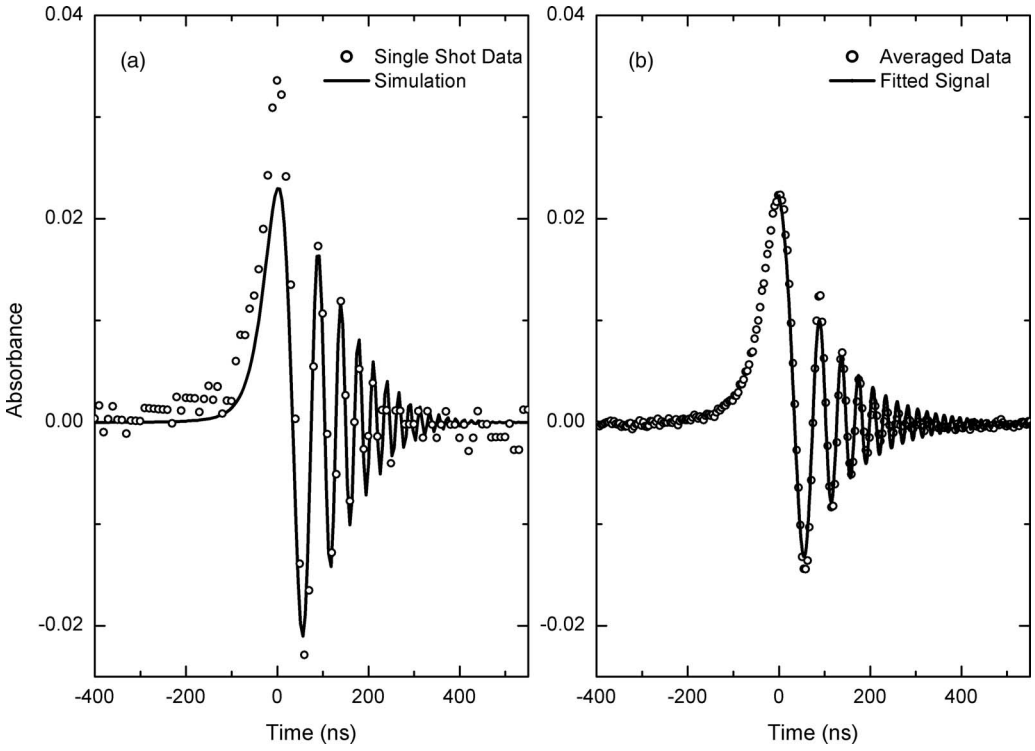

FIG. 4. (a) Rapid passage signal for 50 mTorr of NO obtained at a pump chirp rate of 0.149 kHz ns^{-1} and a single pass of the probe at a scan rate of 145.5 kHz ns^{-1}. The simulated signal given by solving the optical Bloch equations is shown in black. (b) Averaged rapid passage signal for the same conditions as in (a) shown with a fit using Eq. (1). The averaged signal is derived from 50 individual sweeps of the probe laser through resonance.

measured by the probe are directly related to the frequency dependent absorption induced by the sub-Doppler pump laser. When the pump laser is off-resonance with the $R(14.5)_{1/2}$ transition, no transient signal is observed in the probe scan. The bandwidth of the pump laser is sufficiently small compared to the frequency separation between transitions probing different Λ-doublets of the ground rovibrational level that the *e* and *f* components can be considered separately. It can be seen in Figure 3i–iii that there is significant baseline noise as the probe laser is scanned over a range of 1 GHz due to the weak optical feedback from uncoated optics that propagate back into the laser and etalons formed by the front window of the detector. However, the periodicity of these effects is sufficiently different from that of the transient absorption signals to be discriminated and not to affect the conclusions of our work.

Figure 4 shows a zoom in on a single transient signal captured by the probe laser, over a reduced time period of ∼1 μs. The signal shows clear oscillatory structure characteristic of rapid passage. The coherent excitation process (the pump) produces a polarised ensemble of velocity selected molecules. When the probe laser comes into resonance with the pumped velocity group, these vibrationally excited molecules interact with the probe field to generate the transient signal. RP occurs when the probe laser radiation is swept through the molecular transition in a time period which is fast compared with the relaxation time for the system. The probe field then induces an oscillating polarization density within the vibrationally excited subset of molecules which interferes with the electric field of the swept laser radiation and leads to asymmetric absorption profiles.[18]

Experimental evidence supporting the hypothesis that RP is the origin of the oscillatory structure can be found by examining the shapes of the hot band signals both as a function of sample pressure and direction of the laser frequency scan. First, while the signals show a clear free-induction decay type structure at low pressure, this structure is damped at increased pressure due to the dephasing effect of collisions within the measurement time of the experiment, *vide infra*. Second, the decaying signal always occurs post resonance and is independent of the direction of laser scan. Theoretical confirmation of this interpretation is also provided in Figure 4 which shows a comparison between the experimental data and a RP simulation based upon numerically solving the optical Bloch equations.[19] Model inputs include experimentally measured quantities such as laser powers, beam sizes, chirp rates, pump laser bandwidth, population in the vibrationally excited level, and hot band rovibrational transition moment. Further details of the simulation can be found in Ref. 4. The experimental signal is quantitatively well described by the simulation in Figure 4(a), which assumes that the degree of population transfer to the $v = 1$ state is 16% at this pressure, and confirms the occurrence of RP in this system.

To increase the signal to noise ratio of the transient RP signals, an ensemble of traces was averaged over the Doppler absorption profile for each of the probed Λ-doublets using a MATLAB program.[9] The frequency up and down chirp data were separated and the spectra realigned onto the most intense spectral feature to account for small frequency drifts in the probe laser. The averaging does not change either the overall shape of the signal or the decaying oscillations of the RP signals. The averaged RP traces were suitable for fitting in order

to determine the RP decay time and to this aim, the functional form given in Eq. (1) was used, in which μ is half of the probe laser chirp rate and τ is a phenomenological decay constant.[12] The fit of Eq. (1) to the experimental data was made using a Nelder-Mead simplex algorithm to extract a value for τ, as well as the associated errors calculated from the square roots of the diagonals of the covariance matrix,

$$A(t) = A_0 e^{\frac{-t}{\tau}} \sin(\mu t^2). \quad (1)$$

An example of the averaged data is shown in Figure 4(b) and the returned best fit value for τ is 112.4 ± 2.5 ns. The decay rate constant of the RP signal, $(1/\tau)$, is determined by both the decay rate of the population in the upper state and the decay rate of the dipole moment polarisation, with rate constants $1/T_1$ and $1/T_2$, respectively.[7] At pressures of a few tens of mTorr, the average time between collisions is a few μs and is comparable to the time taken for the probe laser to complete one frequency up or down scan. This time period is an order of magnitude longer than the time scale over which RP signals are observed. Therefore the decaying shape of the RP signal is predominantly determined by dephasing of the dipole moment polarisation rather than by collisional relaxation (at least under the experimental conditions of Figure 4).

In order to increase the degree of population transfer and minimise the Doppler dephasing of the RP signal, similar measurements have been conducted for which the function of each laser is reversed, i.e., the DFB become the pump and the EC-QCL is the probe. Due to the limited tunability of the DFB-QCL, the NO transitions used in this case are different to those studied above; the pump laser was tuned to the $R(6.5)_{1/2}$ $v = 1 \leftarrow 0$ transition at 1900.1 cm^{-1} while the probe laser was scanned over the $P(7.5)_{1/2}$ $v = 2 \leftarrow 1$ band at 1822.3 cm^{-1}. The powers of the pump and probe lasers were 201 mW and 116 mW, respectively, and the pressure in the cell was 50 mTorr. In this arrangement the DFB induces ~40% population transfer to the $v = 1$ level, 2.5 times greater than that achieved with the EC-QCL. Varying the power of the pump laser changes both the Rabi frequency for the pump transition and the fraction of molecules pumped into the first vibrationally excited state. To study this effect, the pump operated at a chirp rate of 0.036 kHz ns^{-1} and its power varied in the range 34−202 mW (using a polariser) while the probe was scanned at 225 kHz ns^{-1} with a power of 116 mW. Measurements on a 50 mTorr sample of NO showed that the maximum amplitude of the RP signal varies linearly with pump power while the decay constant remains constant at about (83 ± 4) ns for all pump beam powers. It should also be noted that changing the power of the probe laser did not affect either the magnitude or the decay constant of the transient absorption signals.

B. Effect of laser chirp rate

The effect of varying the chirp rates of both the pump and probe lasers on the RP signals has been investigated. For example, the EC-QCL pump laser (80 mW) was set to scan over the $R(14.5)_{1/2}$ $v = 1 \leftarrow 0$ transition at a rate of 0.149 kHz ns^{-1} while the DFB probe (66 mW) was chirped at a selection of rates within the range 30 to 266 kHz ns^{-1}. As can be seen in Figure 5 the amplitude of the RP signals decreases as the probe chirp rate is increased (Figure 5(a)). Effectively, the probe electric field couples less efficiently to the transition dipole moment for the $R(15.5)_{1/2}$ $v = 2 \leftarrow 1$ hot band transition, resulting in the measured transient absorption being reduced. A similar effect is seen when working with pulsed QCL systems.[20]

The post resonance parts of the transient signals are well fit by Eq. (1) to yield reliable decay constants, τ. The set of measurements shown in Figure 5(b) indicates the decrease of τ as the chirp rate increases and reflects the fact that the probe laser interacts with a progressively larger range of velocity groups per unit time, leading to more rapid Doppler dephasing of the RP signal. Furthermore, as the probe chirp rate increases, τ decreases to a lower limit of ~50 ns; this is the limit imposed by the 20 MHz bandwidth of the detector. The values of the decay constants reported here are significantly larger than those reported by Walker *et al.*[12] (~43 ns for pressures of ≤50 mTorr) as expected due to the smaller linewidth of the probe laser used in this study (800 kHz vs 16 MHz)—the current DFB laser probes a narrower range of velocities and thus the coherent transient signal dephases more slowly.

The corresponding data for the case where the DFB is the pump and the EC-QCL is the probe is shown in Figure 5(c). Here, the pump (201 mW) scan rate was 0.036 kHz ns^{-1}, while the probe (116 mW) was scanned at rates from 20 to 486 kHz ns^{-1}. The decay constant, τ, again decreases as a function of increasing probe laser chirp reaching the aforementioned limit of about 50 ns at the highest chirp rate (Figure 5(d)). However, in this case the limiting value is not reached until the chirp rate is twice as large as before. In addition, the values of τ at low chirp rates are higher than those presented in Sec. III A, e.g., at a chirp rate of 50 kHz ns^{-1} the τ values are 150 ns and 130 ns respectively. The variation of τ with probe laser chirp rate is also smoother than when using the EC-QCL as the pump laser. Both effects directly reflect the narrower linewidth and higher power of the DFB compared to the EC-QCL.

C. Effect of sample pressure

The previously described experiment was repeated at several different NO pressures within the range 7.5 −300 mTorr to investigate the effects of collisional dephasing on the system. In this case, the EC-QCL pump (81 mW) was chirped at 0.149 kHz ns^{-1} and the probe (41 mW) chirped at 145.5 kHz ns^{-1}. As the pressure of NO increases, there are more collisions per unit time and collisions begin to make a greater contribution to the relaxation of the system. Hence, the magnitude of the oscillations within the RP signal decreases and so does the decay time with increased pressure. This behaviour is shown in Figure 6(a) which plots the RP decay time as function of sample pressure for both the *e* and *f* components of the $R(15.5)_{1/2}$ $v = 2 \leftarrow 1$ probe transition. In both cases at low pressure, collisional relaxation is not the limiting factor determining the value of τ but instead it is the spread

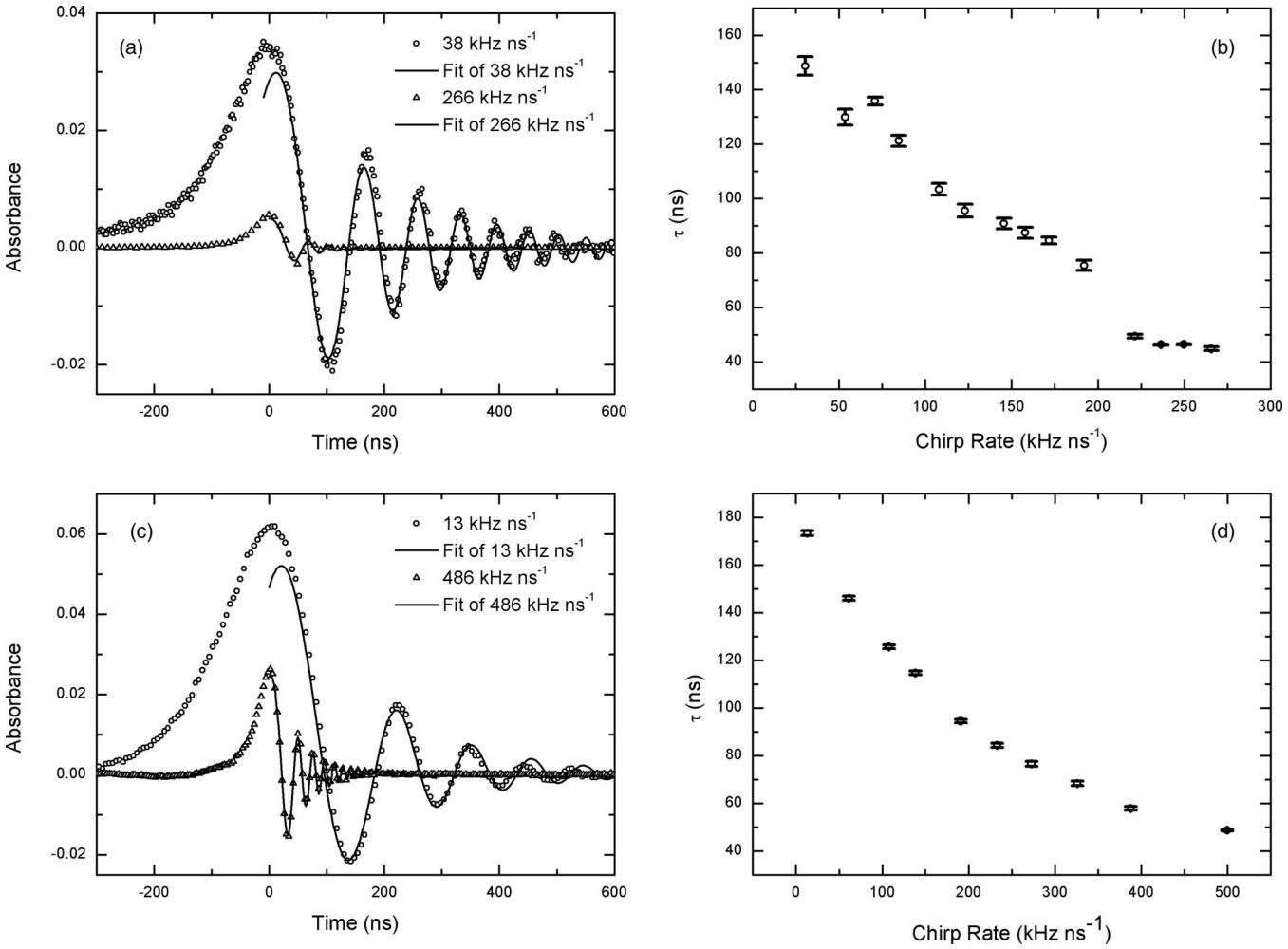

FIG. 5. (a) Rapid passage signals and the corresponding best fits for probe chirp rates of 38 kHz ns^{-1} and 266 kHz ns^{-1} with a pressure of 50 mTorr of NO. (b) Decay constants obtained from the fitting of the experimental rapid passage signals as a function of probe laser chirp rate. (c) Rapid passage signals on the P(7.5)$_{1/2}$ $v = 2 \leftarrow 1$ hot band of NO and their fits taken at 50 mTorr of NO. (d) The decay constants obtained by the fitting of the experimental rapid passage signals as a function of the chirp rate of the probe laser.

of velocities that the probe interacts with. Figure 6 also shows a clear difference in the values of τ for the *e*- and *f* Λ-doublet components (for a fixed pressure) with the RP signals for the *e*-component dephasing faster than those of the *f*-component. The reason for this behaviour is that the three most intense hyperfine components of the transition probing the *e* Λ-doublet are split by a greater amount (0.27 and 0.63 MHz) than the hyperfine components related to the *f*-component (0.21 MHz), giving faster damping of the signal; this interpretation is corroborated by the simulations shown in Figure 6(b). As expected both transitions exhibit the same decay constant in the high pressure limit.

At all of the pressures studied, the Doppler absorption profile of the R(15.5)1/2 $v = 2 \leftarrow 1$ hot band is significantly more intense than that expected from a thermal distribution. Figure 7(a) shows evidence that population is transferred from the initial velocity selected Λ-doublet level into both a range of velocity groups within the same level and into the near-degenerate opposite Λ-doublet level through collisions. If the pump laser is blocked, this background absorption profile disappears. Figure 7(b) shows the Λ-doublet profile of the hot band transition at 59.6 mTorr of NO with the RP signal removed. For comparison, the profile calculated for local thermal equilibrium conditions at the same pressure is also shown. As the pressure is increased the populations of the two Λ-doublet components become more equal, showing the effect of increased collisional energy redistribution. For comparison, in order to observe a maximum absorption of the same magnitude observed at 200 mTorr ($\sim 3 \times 10^{-3}$) without the pump beam, calculation, using absorption cross-section data from the HITRAN database, indicates that the cell would need to be filled with 900 mTorr of NO.[21]

Again, a comparison of the RP signals with the operating roles of the QCLs reversed has been made. For this study, the R(6.5)$_{1/2}$ $v = 1 \leftarrow 0$ transition was pumped with 202 mW of power at a chirp rate of 0.036 kHz ns^{-1}, and the P(7.5)$_{1/2}$ $v = 2 \leftarrow 1$ transition probed with 116 mW at a chirp rate of 226 kHz ns^{-1}. The decay constant found from fitting the resultant RP signals was seen to decrease with increasing pressure as expected due to faster dephasing at higher pressures caused by more frequent collisions. The experiment by Walker *et al.*[12] was performed on the same rovibrational states of NO as this study with the decay constants about half of the ones observed here. Again, this result is directly attributed to

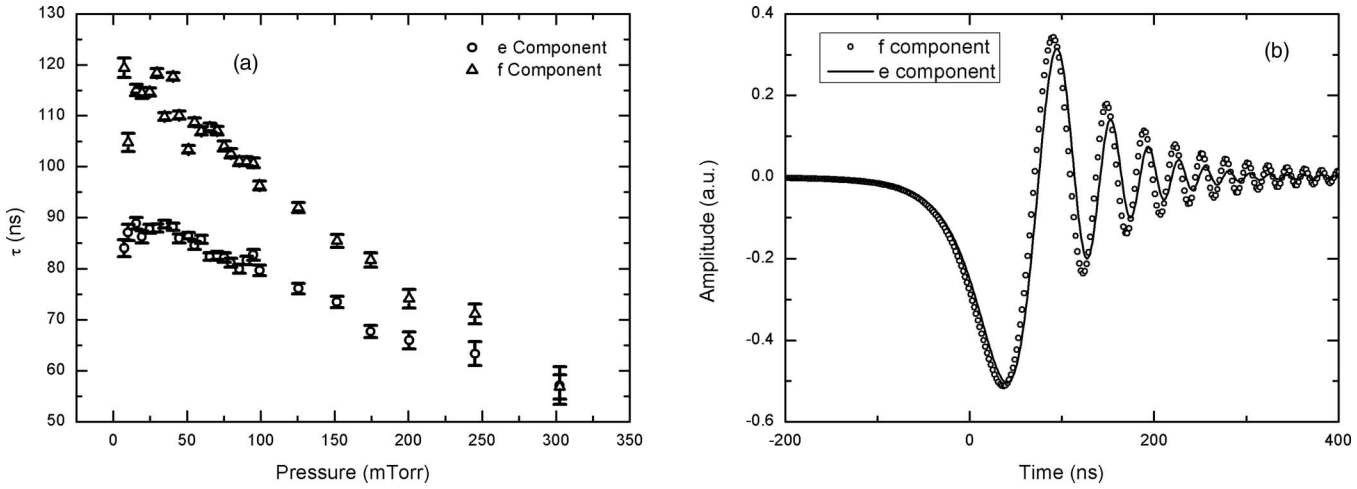

FIG. 6. (a) Decay constants obtained from the fitting of the rapid passage signals as a function of pressure of NO and (b) simulations showing the effect of different hyperfine splitting in the *e* and *f* components of the Λ doublet on the signal decay. The simulations are for a pressure of 20 mTorr and yield decay constants of 89 and 107 ns for the *e* and *f* components, respectively.

the reduced linewidths of both the pump and the probe lasers used here. It is emphasised that both studies observe a plateau at low pressure as in Figure 6, where τ is limited by the range of velocities in the excited state and not by collisional effects.

D. Amplitude modulating the pump pulse: Decay of the transient signal

The data presented above have quantified the temporal decay of the coherent transient absorption signals observed from a velocity selected sample probed with a rapidly swept probe field under conditions of constant pump intensity. In this section, the focus turns to the temporal decay of the coherent transient signal once the pump has been switched off. To this end an AOM was incorporated into the experimental set-up as detailed in Sec. II. The pump frequency was fixed on resonance while the phase of the probe scan was altered in time thereby allowing the velocity selected sample to be probed at a variety of time delays after the AOM has been switched off. Figure 8 shows example data of the coherent transient signals before and after the pump has been extinguished, where the time delay is defined as the period between the pump power falling to half its maximum and the time point corresponding to the maximum amplitude of the coherent transient signal. The data were obtained at a total pressure of 50 mTorr at a chirp rate of 236 kHz ns^{-1} and the signals shown for each time delay are an average of 100 scans. The absorbance values have been normalised in Figure 8 to demonstrate the broadening of the signals at increased time delays. It should be noted that the transient signals shown were obtained towards the end of this study, by which time the performance of the EC-QCL current controller had subtly deteriorated such that its response at high chirp rates was more noisy; the result of this increased noise is that the transient data shown in Figure 8 do not display the marked RP oscillations prevalent in the data obtained under similar conditions earlier and which are presented in Secs. II–IV of the paper (see Figure 5). The veracity of this interpretation has been examined by experiments at lower probe chirp rates (20–100 kHz ns^{-1}) and in all cases the data were very

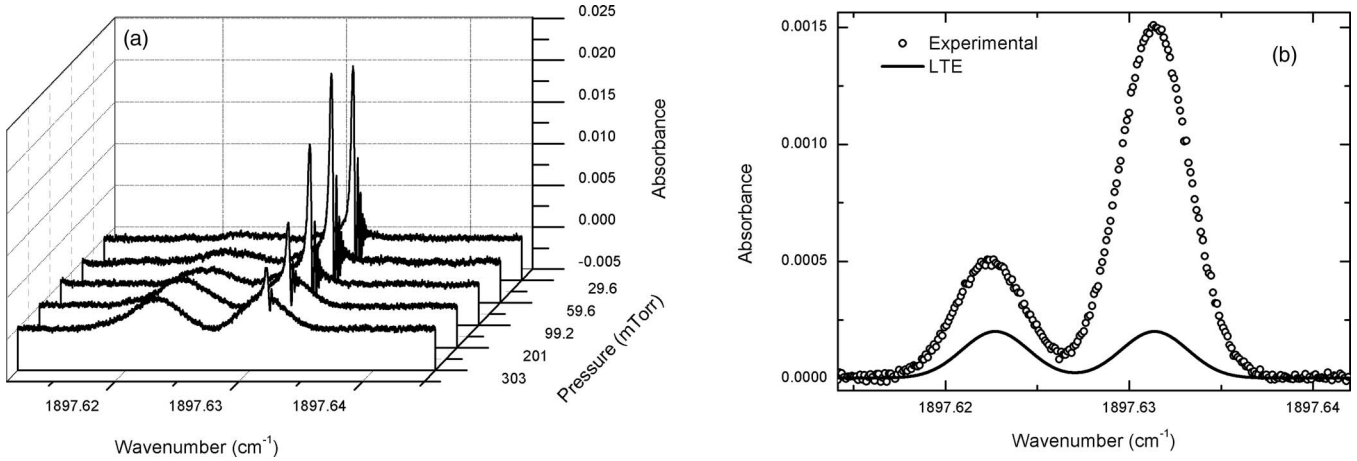

FIG. 7. (a) Absorption profiles of the R(15.5)$_{1/2}$ $v = 2 \leftarrow 1$ hot band transition of NO at different pressures. (b) Doppler profile of the 59.6 mTorr data presented in (a), with the RP signal removed. Also shown in (b) is the calculated absorption profile for the same pressure of NO under local thermal equilibrium (LTE) conditions.

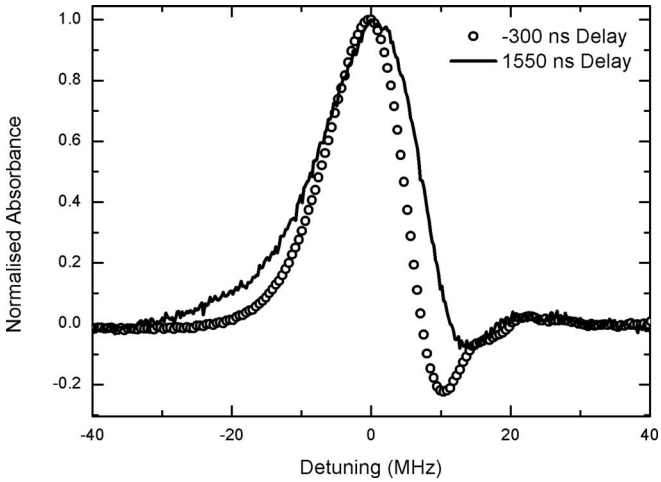

FIG. 8. Coherent transient signals before and after the pump beam has been extinguished. The time delay given is from the point at which the pump power falls to half its maximum to the maximum absorbance of the transient signal.

similar to those presented above and highlight the sensitivity of the measurements to relatively minor changes in the coherence properties of the lasers.

Figure 9 shows the decay of the maximum absorbance and the concurrent increase in the width of the transient signals as a function of time delay, where the width is the full width at half maximum. The amplitude of the signals decay with a time constant of 760 ± 70 ns, reflecting the combined polarization and population relaxation of the system. The linewidth measured while the pump laser is on, is 11.5 MHz and represents the narrow sub-Doppler velocity group prepared by the pump laser which is then broadened by the effective linewidth of the fast-chirping probe laser. The resolution limit, $\Delta\nu$, of a fast chirping laser with a chirp rate μ (Hz s^{-1}) is given by[8,22]

$$\Delta\nu = \sqrt{C\mu}, \tag{2}$$

where C is a constant of order unity. At the measured chirp rate and with a pumped velocity group of 2 MHz width, the effective linewidth of the probe laser is calculated to be 11.3 MHz; this is consistent with a value of C of 0.541 which

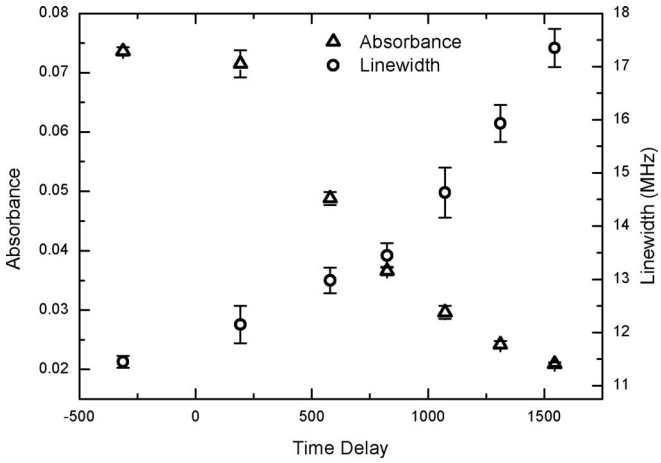

FIG. 9. The evolution of the absorbance and width of the coherent transient signals as a function of time after the pump pulse has been switched off.

falls between the values for Gaussian (0.441) and rectangular time windows (0.886). The observed linewidth of the transient signal is then interpreted as the quadrature sum of the true width of velocity profile in the $v = 1$ state and the effective laser linewidth. The data therefore indicate that the velocity profile in the $v = 1$ state broadens from 2 MHz (while the pump laser is on) to 13 MHz at a time delay of approximately 1.5 μs, i.e., at a rate of 6.45 MHz μs^{-1}. Measurements at 10 mTorr return a linewidth broadening rate that is approximately half this value. These preliminary measurements indicate that similar studies within multi-pass cells are capable of providing details of speed dependent collisional processes. For example, the inherent velocity selection afforded by QCLs can be combined with two colour polarization spectroscopy to provide information about state-to-state differential scattering cross-sections for both elastic and inelastic collisions of vibrationally excited molecules in their ground electronic state, and to measure the degree of polarization retention during inelastic energy transfer.[23,24]

IV. CONCLUSIONS

This paper details results from pump-probe experiments conducted on low pressure samples of NO utilizing two high power cw quantum cascade lasers. The lasers have been tuned to the individual rotationally resolved transitions within the $v = 1 \leftarrow 0$ (pump) and $v = 2 \leftarrow 1$ (probe) vibrational bands and there is clear evidence of velocity selective pumping. The reduced velocity spread in the excited $v = 1$, J, $\Omega = \frac{1}{2}$ states compared to the Doppler width, allowed clear rapid passage structures to be observed in the hot band transient absorption spectra. This conclusion is corroborated by simulations based upon the optical Bloch equations. The effects of altering laser power, chirp rate, and gas pressure in the transient signals were investigated. It is found that the RP signals decay faster in time, i.e., dephases, as both the chirp rate of the probe laser and the pressure of NO was increased indicating that both velocity dephasing and collisional processes are important contributors to the form of the RP signals. The degree of population transfer from the ground state can be quite high, ~40%–45%, and was a maximum with the DFB QCL as the pump, reflecting the reduced bandwidth and higher power of this device compared to the EC-QCL. The use of an acousto-optic modulator to rapidly switch off the QCL excitation allowed the decay time constant for the coherent transient signals to be determined ($\leq$1 μs at 50 mTorr total pressure) as well as its line broadening rate. These initial pump and probe studies highlight the potential utility of the set-up when combined with multi-pass cells, for detailed studies of both inelastic and elastic collisional processes and velocity changing effects, especially given the wide spectral tunability afforded by external cavity QCLs.

ACKNOWLEDGMENTS

This work is conducted under the EPSRC programme Grant No. EP/G00224X/1: New Horizons in Chemical and Photochemical Dynamics.

[1]N. Mukherjee and R. N. Zare, J. Chem. Phys. **132**, 154302 (2010).
[2]N. Mukherjee, C. Kumar, and N. Patel, Phys. Rev. A **80**, 063830 (2009).
[3]N. Mukherjee, J. Chem. Phys. **131**, 164302 (2009).
[4]E. A. McCormack, H. Lowth, M. T. Bell, D. Weidmann, and G. A. D. Ritchie, J. Chem. Phys. **137**, 034306 (2012).
[5]N. Bloembergen, E. M. Purcell, and R. V. Pound, Phys. Rev. **73**, 679 (1948).
[6]M. M. T. Loy, Phys. Rev. Lett. **32**, 814 (1974).
[7]J. C. McGurk, T. G. Schmalz, and W. H. Flygare, J. Chem. Phys. **60**, 4181 (1974).
[8]G. Duxbury, N. Langford, M. T. McCulloch, and S. Wright, Chem. Soc. Rev. **34**, 921 (2005).
[9]J. M. R. Kirkbride, S. K. Causier, E. A. McCormack, D. Weidmann, G. A. D. Ritchie, Phys. Chem. Chem. Phys. **15**, 2684 (2013).
[10]G. Duxbury, J. F. Kelly, T. A. Blake, and N. Langford, J. Chem. Phys. **136**, 174318 (2012).
[11]G. Duxbury, J. F. Kelly, T. A. Blake, N. Langford, J. Chem. Phys. **136**, 174319 (2012).
[12]R. J. Walker, J. H. van Helden, J. Kirkbride, E. A. McCormack, M. T. Bell, D. Weidmann, and G. A. D. Ritchie, Opt. Lett. **36**, 4725 (2011).
[13]T. D. Varberg, F. Stroh, and K. M. Evenson, J. Mol. Spectrosc. **196**, 5 (1999).
[14]L. H. Coudert, V. Dana, J. Y. Mandin, M. Morillon-Chapey, R. Farrenq, and G. Guelachvili, J. Mol. Spectrosc. **172**, 435 (1995).
[15]G. Hancock, G. A. D. Ritchie, J.-P. van Helden, R. Walker, and D. Weidmann, Opt. Eng. **49**, 111121 (2010).
[16]R. J. Walker, J. H. van Helden, and G. A. D. Ritchie, Chem. Phys. Lett. **501**, 20 (2010).
[17]R. J. Walker, J. Kirkbride, J. H. van Helden, D. Weidmann, and G. A. D. Ritchie, Appl. Phys. B **112**, 159 (2013).
[18]S. M. Hamadani, A. T. Mattick, N. A. Kurnit, and A. Javan, Appl. Phys. Lett. **27**, 21 (1975).
[19]H. C. Torrey, Phys. Rev. **104**, 563 (1956).
[20]J. H. van Helden, S. J. Horrocks, and G. A. D. Ritchie, Appl. Phys. Lett. **92**, 081506 (2008).
[21]L. S. Rothman, I. E. Gordon, A. Barbe, D. Chris Benner, P. F. Bernath, M. Birk, V. Boudon, L. R. Brown, A. Campargue, J. P. Champion, K. Chance, L. H. Coudert, V. Dana, V. M. Devi, S. Fally, J. M. Flaud, R. R. Gamache, A. Goldman, D. Jacquemart, I. Kleiner, N. Lacome, W. J. Lafferty, J. Y. Mandin, S. T. Massie, S. N. Mikhailenko, C. E. Miller, N. Moazzen-Ahmadi, O. V. Naumenko, A. V. Nikitin, J. Orphal, V. I. Perevalov, A. Perrin, A. Predoi-Cross, C. P. Rinsland, M. Rotger, M. Šimečková, M. A. H. Smith, K. Sung, S. A. Tashkun, J. Tennyson, R. A. Toth, A. C. Vandaele, and J. Vander Auwera, J. Quant. Spectrosc. Radiat. Transfer **110**, 533 (2009).
[22]B. M. Gorshunov, A. P. Shotov, I. I. Zasavitsky, V. G. Koloshnikov, Yu. A. Kuritsyn, and G. V. Vedeneeva, Opt. Commun. **28**, 64 (1979).
[23]R. J. Wilson and A. J. McCaffery, Chem. Phys. Lett. **261**, 195 (1996).
[24]M. L. Costen and K. G. McKendrick, J. Chem. Phys. **122**, 164309 (2005).